1,3-Dipolar Cycloaddition of Nitrile Oxides to [C60]fullerene: A Density Functional Theory Study

Lydia Rhyman,[a] Sabina Jhaumeer-Laulloo,[a] Luis R. Domingo,[b] John A. Joule,[c] and Ponnadurai Ramasami[a*]

[a] *Department of Chemistry, University of Mauritius, Réduit, Mauritius*

[b] *Departamento de Química Orgánica, Universidad de Valencia, Dr. Moliner 50, 46100 Burjassot, Valencia, Spain*

[c] *The School of Chemistry, The University of Manchester, Manchester M13 9PL, UK*

**Author for correspondence e-mail:* ramchemi@intnet.mu

This paper is presented for

ECSOC-15

International Electronic Conference on Synthetic Organic Chemistry

1-30 November 2011

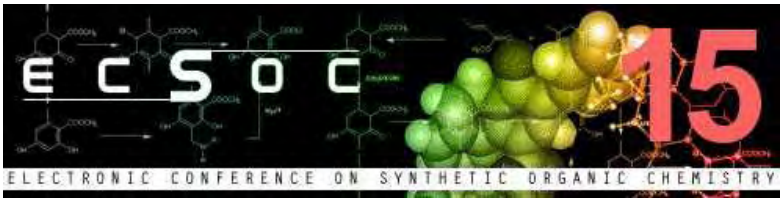

"This presentation is part of the MPhil/PhD research work of Miss Lydia Rhyman (lyd.rhyman@gmail.com, http://www.uom.ac.mu/sites/ccuom/). Her research is based on the theoretical study of cycloaddition reactions and eludication of the reaction mechanisms including different stereo- and regiochemical pathways and to predict the thermodynamic and kinetic parameters of the reactions."

Abstract

The extraordinary structures and properties of fullerenes have had an important impact on nanotechnology as these compounds exhibit outstanding mechanical and electronic properties. 1,3-Dipolar cycloadditions (1,3-DCs) have proved to be a powerful way to functionalize these conjugated π systems and have offered wide opportunities for the creation of new nanocarbon structures with potential application in biological, biotechnology, material science and medicinal chemistry. The 1,3-DCs of fullerene (C_{60}) with nitrile oxides, **RCNO**, have been studied in the gas phase using density functional theory (DFT) at the B3LYP/6-31G(d) level. Energetic and kinetic parameters have been determined at room temperature so as to investigate the effect of electron-withdrawing (**R** = **F**, **Cl**, **Br**, **NC**, **CN** and **NO_2**) and electron-releasing (**R** = **Me** and **Et**) substituents attached to the nitrile oxides on the 1,3-DCs. These parameters have been interpreted in terms of group electronegativity and DFT reactivity indices. An unexpected behaviour was observed for the 1,3-DC involving **FCNO** as these reactions have some pseudodiradical character. Inspired by the results of the 1,3-DCs of nitrile oxides to $C_{60,}$ we have extended this theoretical gas phase research to the addition of a second **HCNO** to the cycloadduct of the addition of **HCNO** on C_{60}. The various possibilities for the second addition are being explored with the aim of determining the thermodynamic and kinetic products. The findings of our research should be helpful to experimentalists in their quests for functionalized fullerenes.

1.0 Introduction

- Fullerene chemistry has become one of the most vigorously developing fields in organic chemistry since the discovery of buckminsterfullerene, C_{60}, by Kroto *et al.*[1] more than two decades ago.

- Fullerene-based materials have found many applications due to the great diversity of functionalizations of the C_{60} spheroid[2] which offer wide opportunities for the creation of new nanocarbons with potential application in biological,[3] material science[4] and medicinal chemistry.[5]

- C_{60} is an electron deficient polyolefin and it is known to undergo various types of reaction such as reductions, halogenations, radical additions, nucleophilic additions, mono- and polycyclic additions.[6]

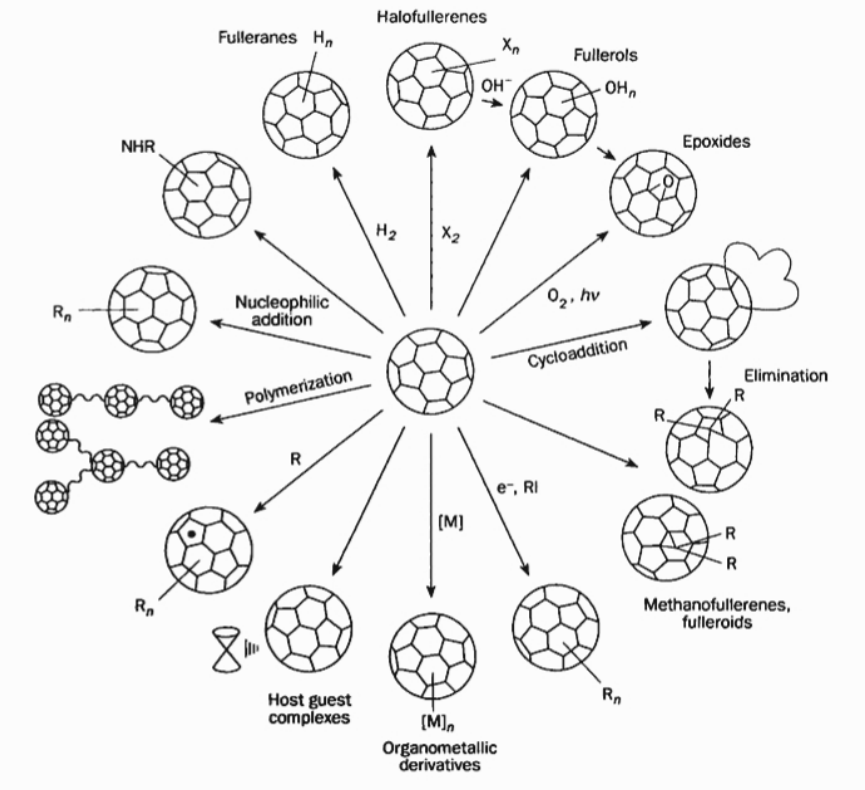

Scheme 1: Different types of reaction observed with C_{60}.[7]

- In the 1990s, several studies revealed that the most employed and straightforward procedures for functionalization of C_{60} are cycloaddition reactions.[8] Of particular interest is the 1,3-DC which plays an important role in the preparation of functionalized C_{60} compounds.

- C_{60} reacts with various nitrile oxides providing a series of fulleroisoxazolines with diverse substitutents (Scheme 2). These fulleroisoxazolines show appealing chemical, electrochemical and photochemical properties.[9]

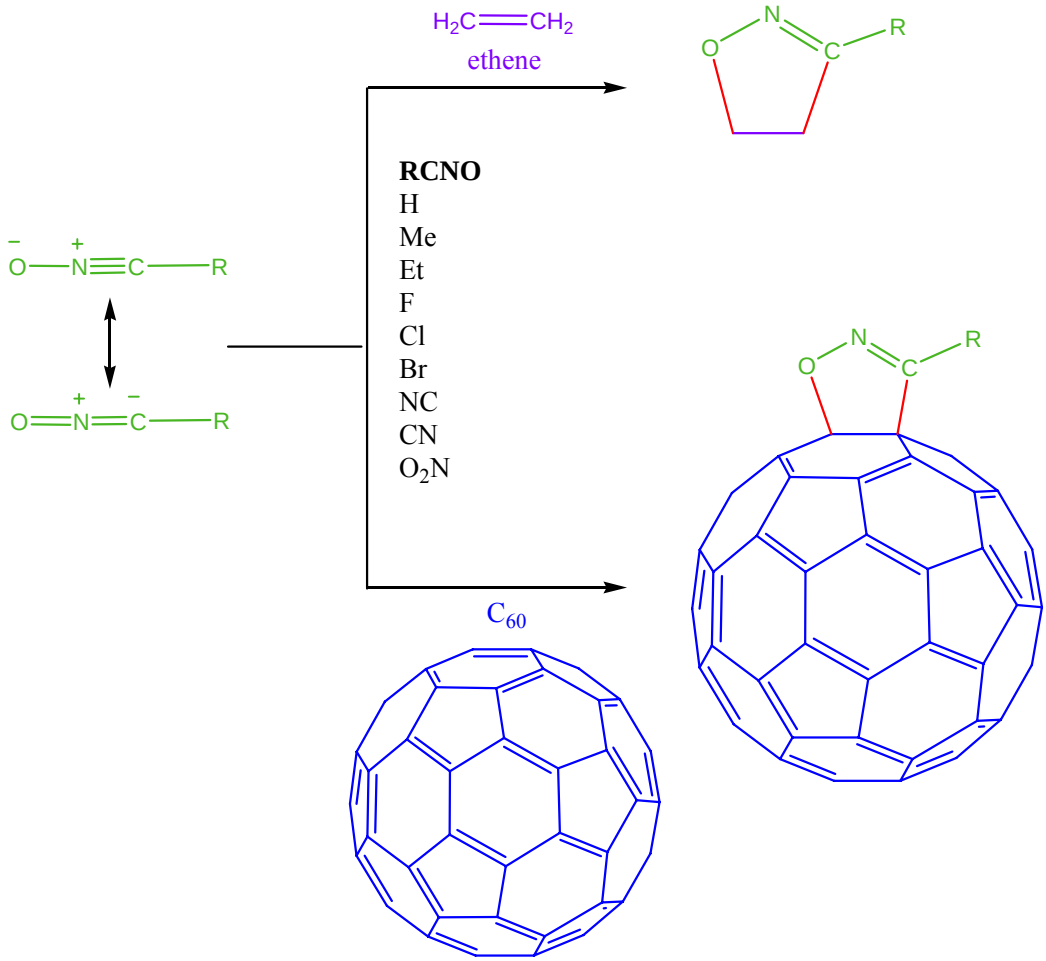

Scheme 2: Model reactions for the 1,3-DC of RCNO with ethene and C_{60}.

- Moreover, it is found that the synthesis of fullerene monoadducts is always accompanied by the formation of diadducts. An understanding of the different possible number of regioisomer bisadducts and their relative stability is important when studying higher functionalized fullerenes.[10]

- Hirsch[11,12] and Wilson[13] groups investigated the diadducts of C_{60} with 1,3-dipoles across the [6,6] position as shown in Figure 1.

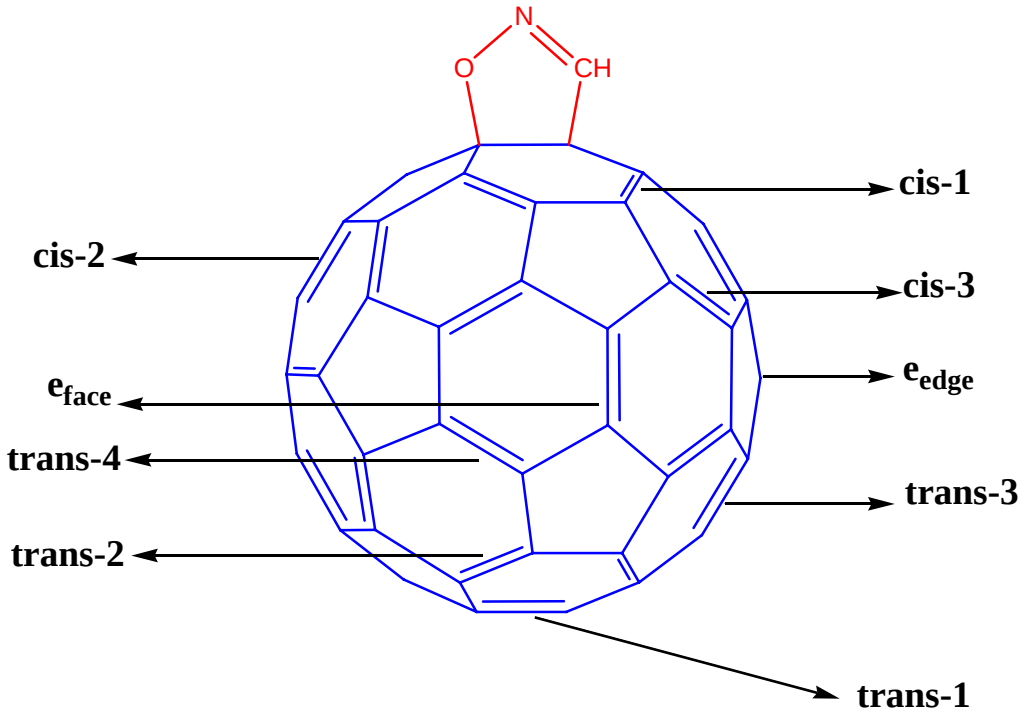

Figure 1: All possible sites of second addition.

1.1 Objectives

- The 1,3-DC of the simplest (**HCNO**) and substituted (**RCNO**) nitrile oxides, with electron-releasing (ER) substitutents (**R** = **Me** and **Et**) and electron-withdrawing (EW) substituents (**R** = **F**, **Cl**, **Br**, **NC**, **CN** and **NO_2**), with C_{60} (Scheme 2) is studied by means of B3LYP/6-31G(d) computations. For comparison, the 1,3-DC of these nitrile oxides to ethene have also been studied.

- The energetic, thermodynamic and kinetic parameters of these reactions are investigated.

- The features of the reaction mechanism such as synchronicity, nature of transition state structure (TS), charge transfer (CT), analysis of the reactivity indices and the rate constants of these 1,3-DCs are also taken into consideration.

- The second addition of the **HCNO** to its monoadduct is also being considered at the same level of theory. Here, the 1,3-dipole is unsymmetrical and thus, we analyze all the possible regioisomers.

2.0 Results and discussion

2.1 Energetics

- 1,3-DC can occur at a [6,6] or a [5,6] bond of C_{60} and can form closed and open CAs. Therefore, the reaction can proceed through four types of additions; closed [6,6], closed [5,6], open [6,6] and open [5,6]. However, only the closed [6,6] concerted pathway is taken into consideration as it leads to the most stable CA as supported by various studies.[18]

- In general, the presence of ER groups on the 1,3-dipole increases the activation energy compared to the EW groups (Table 1). Moreover, the activation energy drastically decreases when **R** = **F**.

Table 1: Relative energies[a] (kJ mol^{-1}) including ZPE computed at 298.15 K and 1 atm for the reactions of **RCNO** with ethene and C_{60}.

R	**H**	**Me**	**Et**	**F**	**Cl**	**Br**	**NC**	**CN**	**NO_2**
				RCNO + $H_2C=CH_2$					
TS	55.7	58.2	56.9	6.5	30.5	36.6	49.7	31.3	16.2
CA	-166.7	-160.4	-159.6	-270.7	-214.7	-201.1	-167.4	-205.3	-239.9
				RCNO + C_{60}					
TS	51.6	49.5	48.1	5.8	29.7	32.6	53.8	32.9	17.5
CA	-104.9	-101.3	-100.7	-207.9	-148.4	-139.6	-98.2	-138.0	-166.1

[a] *Relative to **RCNO** + ethene or **RCNO** + C_{60}.*

- The predicted activation energy has been correlated with electronegativity of the substituent on the nitrile oxides based on the Pauling electronegativity scale and 'super-atom' approximation[19] (Figure 2).

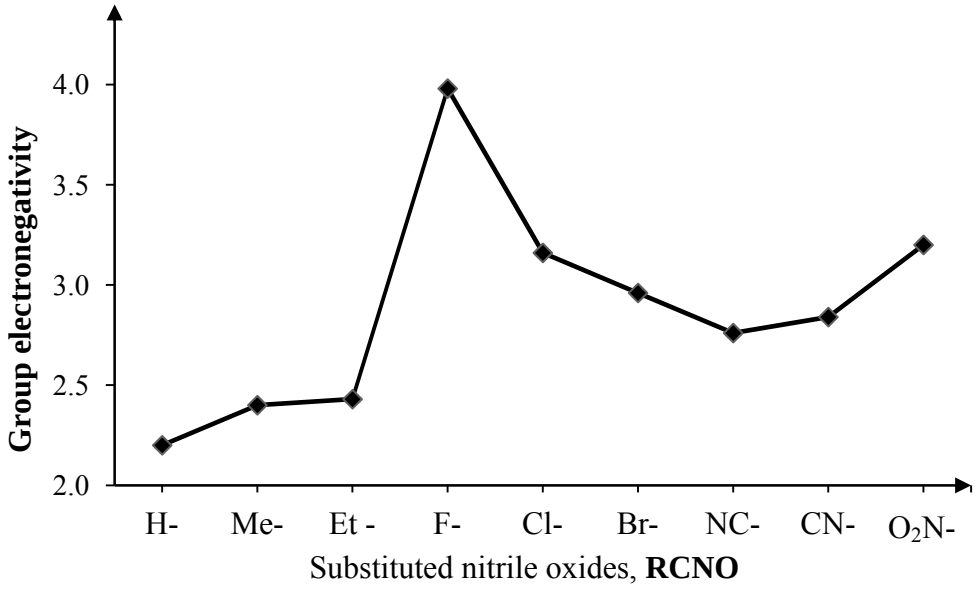

Figure 2: Group electronegativity of the substituent on the nitrile oxides.

- It can be observed that the predicted activation energy is inversely proportional to the group electronegativity as illustrated in Figure 3.

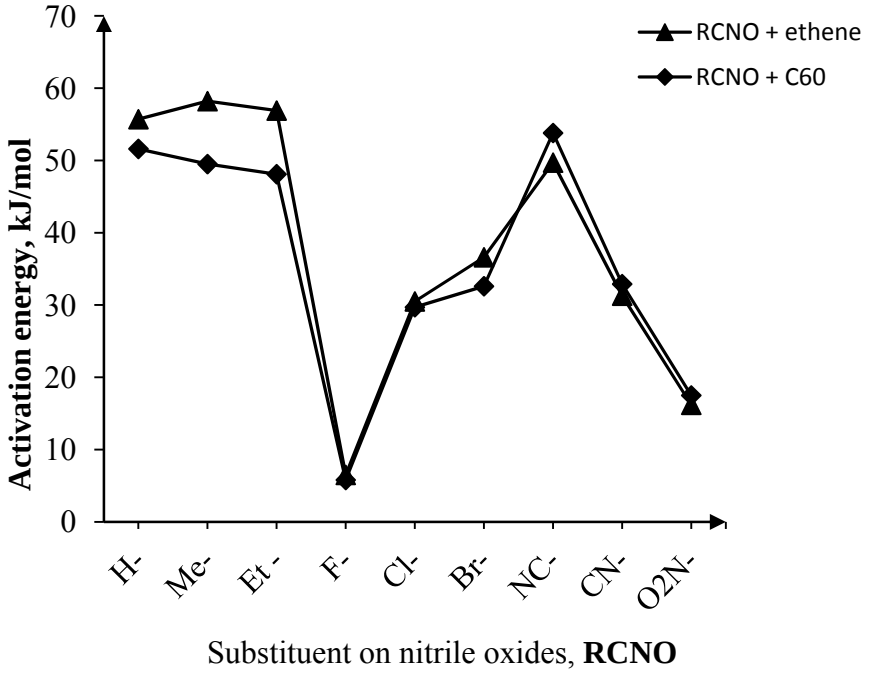

Figure 3: Activation energy for the 1,3-DC of nitrile oxides with ethene and C_{60}.

2.2 Geometrical Parameters of Transition States

- An analysis of the geometries of the TSs (Figures 4 and 5) associated with these 1,3-DCs show that these reactions are asynchronous concerted processes.

- Analysis of the lengths of the two forming bonds at the TSs indicates that the length of the C–O forming bond is longer than the C–C bond, suggesting that the formation of C–C bond is more advanced than the C–O bond.

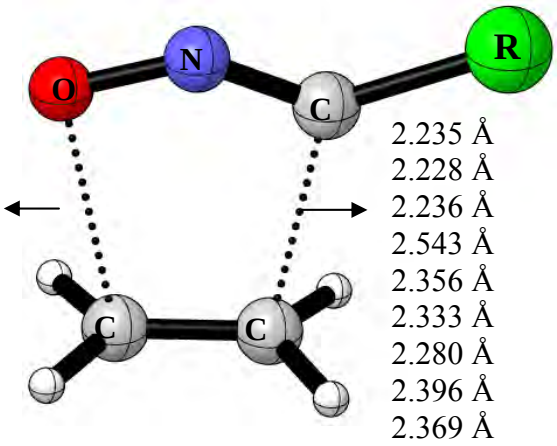

RCNO		
H-	2.413 Å	2.235 Å
Me-	2.351 Å	2.228 Å
Et-	2.356 Å	2.236 Å
F-	2.582 Å	2.543 Å
Cl-	2.469 Å	2.356 Å
Br-	2.446 Å	2.333 Å
NC-	2.405 Å	2.280 Å
CN-	2.467 Å	2.396 Å
O_2N-	2.644 Å	2.369 Å

Figure 4: Optimized geometries of the TSs involved in the 1,3-DCs between nitrile oxides with ethene.

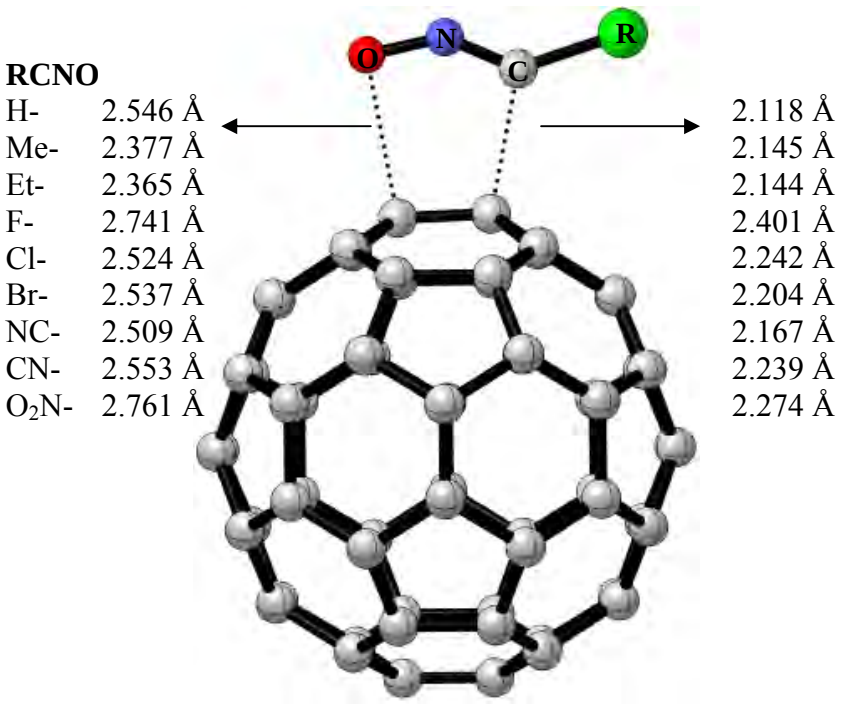

Figure 5: Optimized geometries of the TSs involved in the 1,3-DCs between nitrile oxides with C_{60}.

- The degree of asynchronicity, Δ*d*, can be determined by considering the ratio of difference between the lengths of the two forming bonds such that Δ*d* = [d(C–O) – d(C–C)] as shown in Table 3. Greater asynchronicity is observed for the 1,3-DC of nitrile oxide with C_{60} than with ethene, which is due to the polarity of both the 1,3-dipoles and dipolarophiles.

Table 3: *Δd* at the TSs arising from the 1,3-DC of **RCNO** with ethene and C_{60}.

R	**H**	**Me**	**Et**	**F**	**Cl**	**Br**	**NC**	**CN**	**NO_2**
RCNO + $H_2C=CH_2$									
Δ*d*	0.18	0.12	0.10	0.04	0.11	0.11	0.13	0.07	0.28
RCNO + C_{60}									
Δ*d*	0.43	0.23	0.25	0.34	0.28	0.33	0.34	0.31	0.49

2.3 Bond Order and Charge Transfer

- The Wiberg bond indices[14] have been computed to follow the nature of the cycloaddition process using NBO analysis.

- The bond order (BO) values for the C–C forming-bond at the TSs (Table 4) are larger than those for the C–O bond. For the 1,3-DCs with C_{60}, while the C–C BO values increase relative to those in the reactions with ethene, the C–O decrease, indicating that the TSs are more advanced and more asynchronous.

- It is noteworthy that the presence of an EW group on the nitrile oxide results in a low BO value for both the C–O and C–C bond formation processes.

Table 4: Wiberg bond orders of the TSs involved during the 1,3-DC of nitrile oxides with ethene and C_{60}.

	RCNO + $H_2C=CH_2$		**RCNO + C_{60}**	
	C–O	C–C	C–O	C–C
HCNO	0.21	0.30	0.14	0.33
MeCNO	0.22	0.30	0.18	0.32
EtCNO	0.22	0.29	0.18	0.32
FCNO	0.12	0.15	0.08	0.17
ClCNO	0.17	0.22	0.13	0.25
BrCNO	0.19	0.24	0.13	0.27
NCCNO	0.20	0.26	0.14	0.30
CNCNO	0.17	0.22	0.12	0.25
O_2NCNO	0.13	0.19	0.08	0.24

- The electronic nature of these 1,3-DCs is evaluated by analyzing the CT at the TSs. The natural atomic charges are shared between the nitrile oxides and the dipolarophiles, ethene and C_{60}, and these data are shown in Table 5. For the reactions with ethene, the natural population analysis gives a negligible CT, pointing out non-polar processes with some pseudodiradical character.[15,16]

- It is to be noted that CT increases slightly with the EW character of the substituent. The 1,3-DCs with C_{60}, also present very low CT; however, at these cycloadditions, the flux of the electron density depends on the nature of the substituent present on nitrile oxide. Thus, while for the ER **Me** and **Et** groups the CT fluxes towards C_{60}, for the EW **CN** and **NO_2** groups the CT fluxes towards the nitrile oxide.

Table 5: Charge transfer (CT, in e), dipole moment (DM, in Debye) and imaginary frequency (IF, in cm^{-1}) of TSs.

R	**H**	**Me**	**Et**	**F**	**Cl**	**Br**	**NC**	**CN**	**NO_2**
				RCNO + H_2C=CH_2					
CT	-0.02	-0.01	-0.01	-0.02	-0.04	-0.05	-0.08	-0.05	-0.07
DM	2.462	3.250	3.310	1.465	1.788	2.009	2.542	1.588	2.322
IF	-406.3	-407.4	-389.2	-170.8	-304.9	-319.5	-367.8	-301.6	-241.7
				RCNO + C_{60}					
CT	0.05	0.08	0.08	0.01	0.01	0.02	-0.05	-0.02	-0.07
DM	2.127	3.222	3.489	1.364	1.584	1.960	2.997	1.797	3.121
IF	-400.3	-388.6	-361.3	-137.4	-301.9	-326.2	-371.6	-301.7	-229.0

- All TSs have only one imaginary vibrational frequency, corresponding to the atomic motion along the direction of the newly forming bonds. The imaginary frequency values for the ER substituted nitrile oxides are slightly lower than for the EW substituted ones. These low values indicate that these processes are associated with heavy atom motions and are also related to the earlier TSs.

2.4 Reactivity Indices

- Recent studies[17-19] carried out on cycloaddition reactions have shown that the reactivity indices defined within the conceptual DFT are powerful tools for establishing the polar character of such reactions. Table 6 lists the static global properties.

Table 6: Electronic chemical potential (μ), chemical hardness (η), global electrophilicity (ω), and global nucleophilicity (N), in eV, of C_{60}, ethene and substituted nitrile oxides.

	μ	η	ω	N
C_{60}	-4.61	2.76	3.84	3.13
O_2NCNO	-5.97	4.70	3.79	0.80
FCNO	-4.92	5.05	2.40	1.67
NCCNO	-5.26	6.09	2.27	0.82
CNCNO	-4.84	5.96	1.96	1.30
ClCNO	-4.26	5.98	1.52	1.87
BrCNO	-4.15	5.83	1.48	2.06
Ethene	-3.37	7.76	0.73	1.87
HCNO	-3.40	7.94	0.73	1.75
EtCNO	-2.91	7.51	0.56	2.46
MeCNO	-2.90	7.66	0.55	2.39

- The electronic chemical potential of C60 is μ = -4.61eV. On the other hand, for the nitrile oxides the electronic chemical potential ranges from μ = -2.90 eV for **MeCNO** to μ = -5.97 eV for **O_2NCNO**. Therefore, it is expected that in a polar process the flux of the CT depends on the nature of the substituent present on nitrile oxide. The electrophilicity of C_{60}, ω = 3.84 eV, allows for the classification of this species as a strong electrophile within the electrophilicity scale.[17]

- On the other hand, a high nucleophilicity value, N = 3.13 eV, is predicted for C_{60} and thus, it is classified a strong nucleophile within the nucleophilicity scale.[20] Ethene has low electrophilicity and nucleophilicity values, ω = 0.73 eV and N = 1.87 eV. Therefore, it is expected that ethene does not participate in polar processes, in clear agreement with the low CT found in these 1,3-DCs.

- A good correlation can be found between the EW or ER character of the substituent and the electrophilicity of the corresponding nitrile oxide. Thus, while **O_2NCNO** is the most electrophilic, **MeCNO** is the poorest electrophilic nitrile oxide. In general the increase of the

electrophilic character of the nitrile oxide can be related with the decrease of the nucleophilic one.

- Analysis of the CT at the TSs of the 1,3-DCs with C_{60}, indicates that they take place with a low polar character. In spite of this behavior, if the faster reaction, **FCNO**, and the slowest one, **NCCNO**, are discarded from the series, a reasonable correlation is found between the electrophilicity of nitrile oxide **RCNO** and the activation energy of the 1,3-DC with $R^2 = 0.87$ as illustrated in Figure 6.

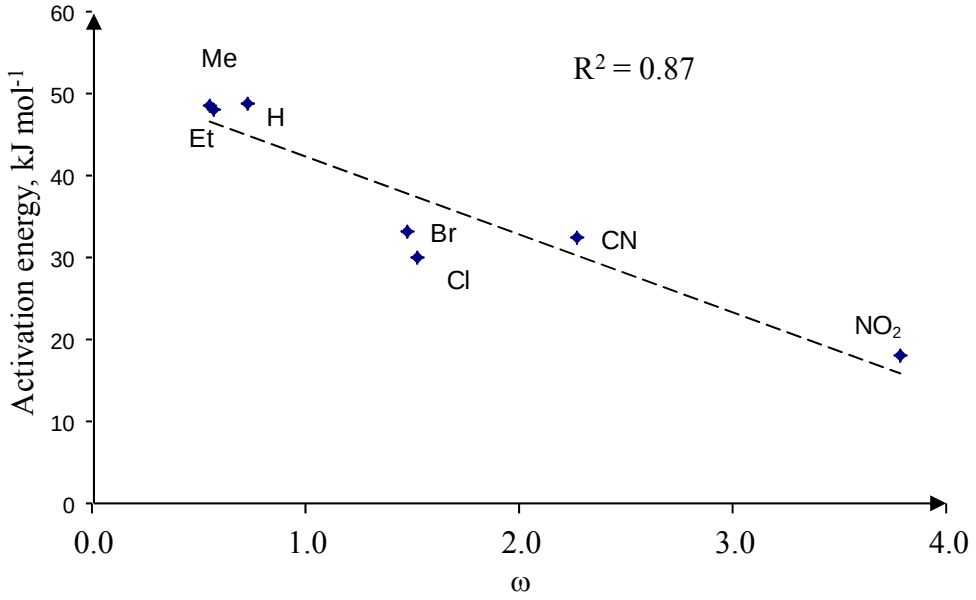

Figure 6: Plot of the activation energies (ΔE^a, in kJ/mol) associated with the 1,3-DCs of some substituted nitrile oxides with C_{60} *versus* the electrophilicity ω of the nitrile oxide.

- In addition, considering the electronic chemical potential of C_{60}, we can explain the change of the flux of the CT on the 1,3-DC reactions included in Figure 6 (see Table 5); **O_2NCNO** (-5.97 eV) < **NCCNO** (-5.26 eV) < C_{60} (-4.61 eV) < **ClCNO** (-4.26 eV) < **BrCNO** (-4.15 eV) < **HCNO** (-3.40 eV) < **EtCNO** (-2.91 eV) < **MeCNO** (-2.90). Thus, while for the 1,3-DCs

with; **O_2NCNO** and **NCCNO** the charge fluxes from C_{60}, to these nitrile oxides, for the rest the charge fluxes towards C_{60}.

- At this stage, it is interesting to comment on the 1,3-DCs with **FCNO**. The cycloadditions of this nitrile oxide with ethene and C_{60} are the fastest reactions, in spite of being a weaker electrophile than **O_2NCNO**. On the other hand, these reactions show the lowest CT, pointing to non-polar processes. These behaviors suggest that the 1,3-DCs of **FCNO** can take place through earlier TSs with some pseudodiradical character,[26] which could be favored by the presence of the fluorine atom.

- Although C_{60} has larger electrophilicity and nucleophilicity values than ethene (See Table 6), the comparable relative energies and the low CT for 1,3-DCs of these dipolarophiles with the **RCNO** series indicate that, like ethene,[23] the 1,3-DCs of C_{60} have non-polar character. Despite of its pseudodiradical character, C_{60} appears to have some response to the electrophilic/nucleophilic behavior of **RCNOs** as shown Figure 5.

2.5 Rate Constants

- The rate constants for the second order elementary step, k_1 for the 1,3-DCs of the nitrile oxides with ethene and C_{60} are reported in Table 7. Our calculations show that $k_2 >> k_{-1}$ and thus, from equation (2), the effective rate constant k_{ef} is same as k_1. On comparing the 1,3-DC with ethene and C_{60} with nitrile oxides it is found that the larger rate constants, k_1, are associated with ethene.

- The rate constant increases in the order **Et** < **Me** < **H** < **NC** < **Cl** < **Br** < **NO_2** < **CN** < **F** for the reaction between **RCNO** with ethene and **Et** < **H** < **Me** < **NC** < **Cl** < **NO_2** < **CN** < **Br** < **F** for

the reaction between **RCNO** with C_{60}. Thus, the reaction with **FCNO** is fastest compared to reaction with the other nitrile oxides.

- In general, the variations in the rate constants can be rationalized in terms of activation energies. It is important to note that there is a good agreement with the values of the k_1 calculated from equations (3) and (6).

Table 7: Rate constants, k_1, of the 1,3-DCs of nitrile oxides with ethene and C_{60}.

RCNO	**RCNO + $H_2C=CH_2$**		**RCNO + C_{60}**	
	$k_1{}^a$	$k_1{}^b$	$k_1{}^a$	$k_1{}^b$
H	1.90	2.20	1.02	1.18
Me	4.95×10^{-1}	5.74×10^{-1}	1.04	1.19
Et	1.86×10^{-1}	2.12×10^{-1}	3.45×10^{-1}	3.88×10^{-1}
F	$6.01 \times 10^{+8}$	$6.17 \times 10^{+8}$	$8.82 \times 10^{+7}$	$9.75 \times 10^{+7}$
Cl	$2.39 \times 10^{+4}$	$2.60 \times 10^{+4}$	$1.82 \times 10^{+3}$	$1.98 \times 10^{+3}$
Br	$9.38 \times 10^{+5}$	$1.03 \times 10^{+6}$	$2.28 \times 10^{+5}$	$2.51 \times 10^{+5}$
NC	$8.34 \times 10^{+2}$	$9.42 \times 10^{+2}$	9.44	10.68
CN	$6.26 \times 10^{+6}$	$6.79 \times 10^{+6}$	$2.22 \times 10^{+5}$	$2.41 \times 10^{+5}$
NO_2	$2.19 \times 10^{+6}$	$2.31 \times 10^{+6}$	$2.77 \times 10^{+4}$	$2.91 \times 10^{+4}$

[a] *k_1 calculated from equation (3)*
[b] *k_1 calculated from equation (6)*

2.6 Second addition of HCNO to monoadduct

- The second addition of HCNO to the *cis*-1 position of the monoadduct of C_{60} has two possibilities depending on the orientation of the oxygen atom, *syn* and *anti*. The *syn* addition of **HCNO** is first considered and is displayed in Figure 7 along with the activation energy (E^a) and reaction energy (ΔE).

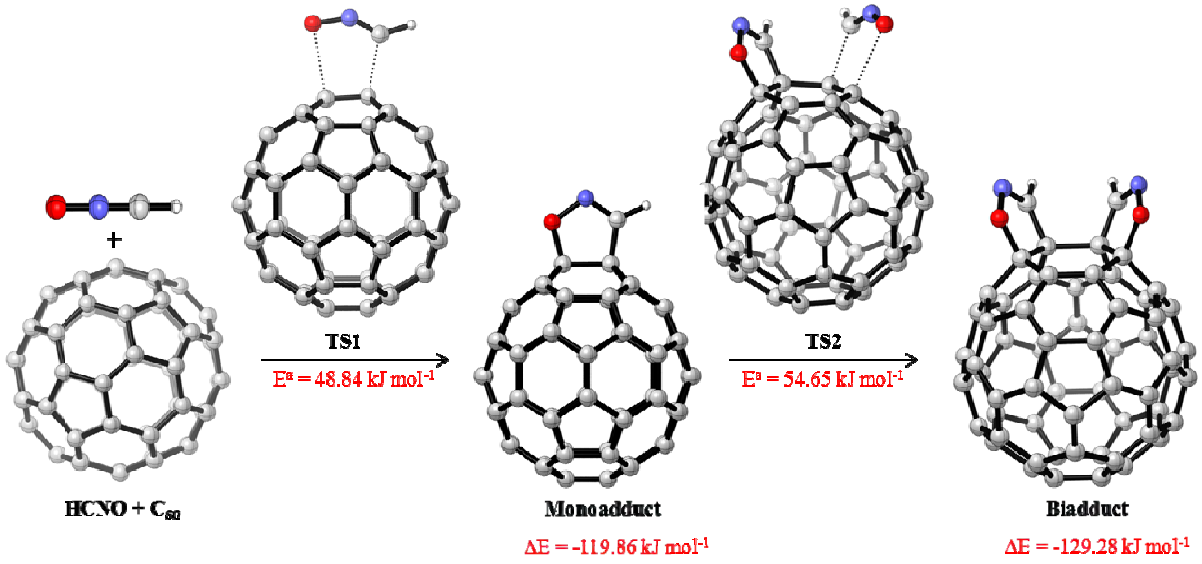

Figure 7: Reaction profile of the *syn* addition of **HCNO** on the *cis*-1 position of monoadduct C_{60}.

- The *anti* addition at the *cis*-1 position is illustrated in Figure 8.

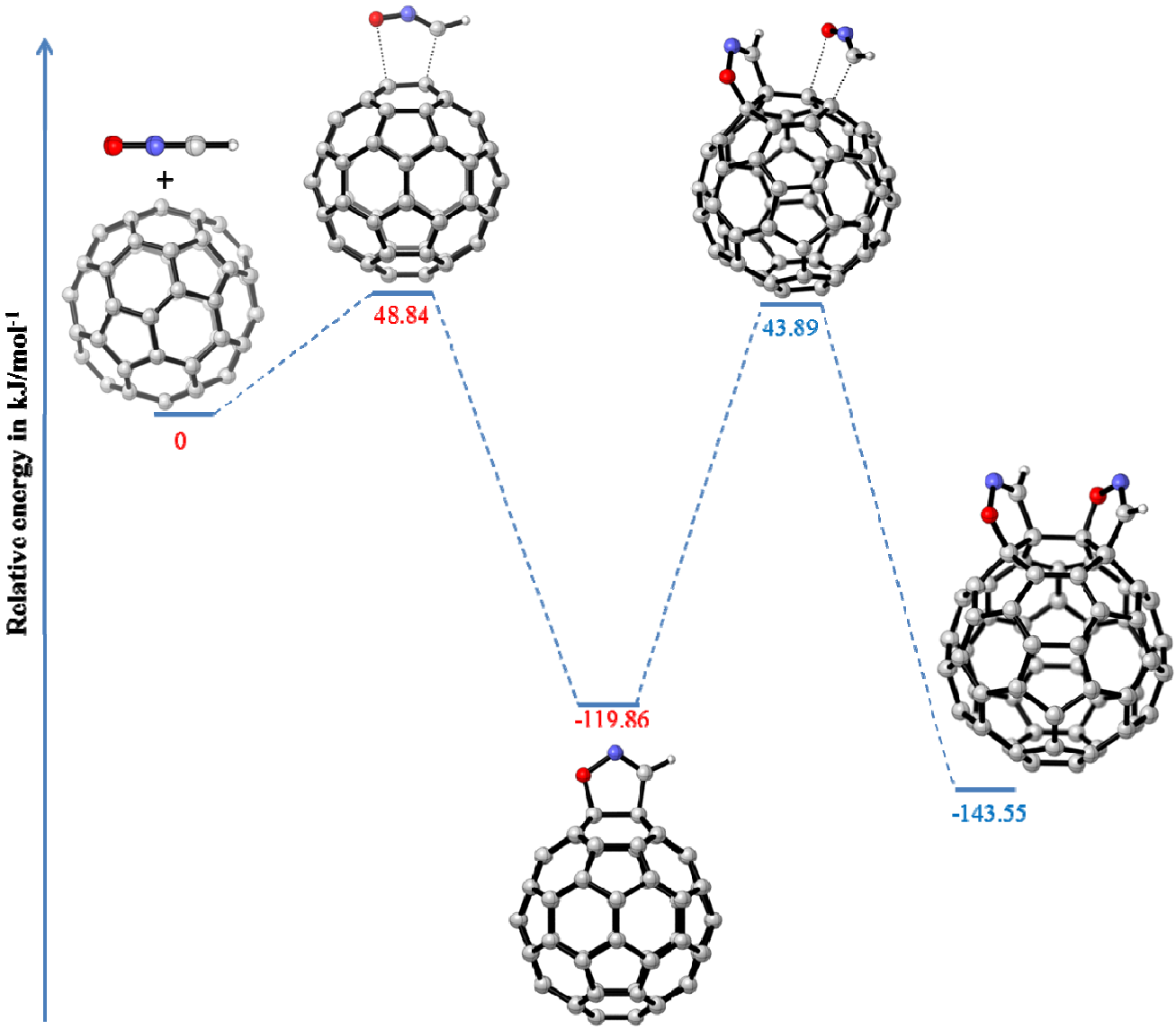

Figure 8: Reaction profile of the *anti* addition of **HCNO** on the *cis*-1 position of monoadduct C_{60}.

- Currently, we are investigating other possibilities.

3.0 Methodology

- Gas phase full geometries optimizations have been carried out using the B3LYP functional with the 6-31G(d) basis set.

- Harmonic vibrational analysis was performed to verify each minimum on the potential energy surface.

- The intrinsic reaction coordinate[21,22] (IRC) path was traced, at the same level of theory, to ensure that the TSs led to the expected reactants and products.

- Natural bond orbital (NBO) analysis was performed on the electronic structures of the critical points according to Weinhold and coworkers[23,24] as implemented in Gaussian 03.[25]

- The global electrophilicity index, ω, is calculated following the expression,[26-28] $\omega = (\mu^2/2\eta)$, where μ is the electronic chemical potential ($\mu \approx (\varepsilon_H + \varepsilon_L)/2$) and η is the chemical hardness $\eta \approx (\varepsilon_L - \varepsilon_H)$.

- The nucleophilicity index, N,[29] which we have recently introduced is defined as $N = \varepsilon_{H(Nu)} - \varepsilon_{H(TCE)}$ where tetracyanoethylene (TCE) is chosen as the reference. This choice allowed us conveniently to handle a nucleophilicity scale of positive values.[30]

- The rate constant, calculated at 298.15 K, is predicted according to the following equation (1):

$$\mathbf{1 + 2} \underset{k_{-1}}{\overset{k_1}{\rightleftharpoons}} \mathbf{TS} \xrightarrow{k_2} \mathbf{CA} \qquad (1)$$

- The effective rate constant corresponding to the formation of CAs can, thus, be calculated as:

$$k_{ef} = \frac{k_1 k_2}{k_{-1} + k_2} \qquad (2)$$

- The rate constant of each step is calculated based on the conventional transition state theory[31-33] (TST) equations:

$$k_1 = \kappa \frac{k_B T}{h} \frac{RT}{p} exp \frac{\Delta S^\circ}{R} exp\left(-\frac{\Delta H^\circ}{RT}\right) \quad (3)$$

$$k_{-1} = \kappa \frac{k_B T}{h} exp\left(-\frac{\Delta S^\circ}{R}\right) exp \frac{\Delta H^\circ}{RT} \quad (4)$$

$$k_2 = \kappa \frac{k_B T}{h} exp\left(\frac{\Delta S^{\neq}}{R}\right) exp\left(-\frac{\Delta H^{\neq}}{RT}\right) \quad (5)$$

where k_B is Boltzmann's constant; h is Planck's constant, T is the temperature; R is the ideal gas constant; κ is the transmission coefficient and is taken to be 1; ΔH° is the relative enthalpy, $\Delta H^{\neq}$ is the activation enthalpy while ΔS° and $\Delta S^{\neq}$ are the relative and activation entropies, respectively.

- The rate constant, k_1, has also been calculated with the Wigner tunneling coefficient[38c,39] according to the standard Eyring TST as:

$$k_1 = \Gamma \frac{k_B T}{h} \frac{Q_{TS} N_A}{Q_1 Q_2} exp\left(-\frac{\Delta E_a}{RT}\right) \quad (6)$$

where N_A is the Avogadro's number; Q_{TS}, Q_1 and Q_2 are the total partition functions of TS, **1** and **2**, respectively and ΔE_a is the activation energy for the cycloaddition. The values of the rate constants are calculated at standard conditions (T = 298.15 K and p = 101325 Pa).

4.0 Conclusions and Future Work

- The influence of EW and ER substituents on the 1,3-DC reactivity of C_{60} has been determined in the closed [6,6] pathway in the gas phase. The activation energies for the reaction of **RCNO** + ethene follow the order **R** = **F** < **NO_2** < **Cl** < **CN** < **Br** < **NC** < **H** < **Et** < **Me**, which is in agreement with the reaction **RCNO +** C_{60}, **R** = **F** < **NO_2** < **Cl** < **CN** < **Br** < **Et** < **Me** < **H** < **NC**, with only **NC** misplaced.

- The geometrical parameter and BO analysis reveal that the TSs are concerted and asynchronous. Moreover, the presence of an EW group on the nitrile oxide results in more asynchronous TSs and the more ER group go through more synchronous TSs.

- In spite of the low CT found in these 1,3-DCs, a good correlation between the electrophilicity of the nitrile oxide and the activation energy of the reaction is found; the increase of the electrophilicity of **RCNO** accelerates the reaction towards a C_{60} to nitrile oxide CT process. Finally, the 1,3-DCs of **FCNO**, *via* the less polar TSs, are the fastest reactions. This behavior can be associated with some pseudodiradical character of the cycloaddition, raised by the presence of fluorine substituent.

- We look forward that these aforementioned data will be helpful to experimentalists in their attempts for the synthesis and characterization of these novel compounds.

- As future work, we will analyze the other conceivable biadducts and discuss their relative stability.

Acknowledgements

Computational facilities offered by Institute of Physical Chemistry of Romanian Academy and from University of Mauritius are acknowledged. This work was supported by funding provided by the Mauritius Tertiary Education Commission (TEC). The organizing committee of the 15th ECSOC is also acknowledged.

References

1. Kroto, H. W.; Heath, J. R.; O, B., S. C.; Curl, R. F.; Smalley, R. E. *Nature* **1985,** 318, 162.

2. Yurovskaya, M. A.; Trushkov, I. V. *Russ. Chem. Bull. Int. Ed.* **2002,** 51, 367.

3. Markovic, Z.; Trajkovic, V. *Biomaterials* **2008,** 29, 3561.

4. Prato, M. *Top. Curr. Chem.* **1999,** 199, 173.

5. Maeda-Mamiya, R.; Noiri, E.; Isobe, H.; Nakanishi, W.; Okamoto, K.; Doi, K.; Sugaya, T.; Izumi, T.; Homma, T.; Nakamura, E. *Proc. Natl. Acad. Sci.* **2010,** 107, 5339.

6. Hirsch, A.; Brettreich, M. Fullerenes: Chemistry and Reactions; Wiley-VCH Verlag GmbH & Co. KGaA: Weinheim, 2005.

7. Roger, T.; Walton, D. R. *Nature* **1993,** 363, 685.

8. Hirsch, A. *Synthesis* **1995**, 895.

9. Yang, H.-T.; Ruan, X.-J.; Miao, C.-B.; Sun, X.-Q. *Tetrahedron Lett.* **2010,** 51, 6056.

10. Irngartinger, H.; Fettel, P. W. *Tetrahedron* **1999,** 55, 10735.

11. Hirsch, A.; Lamparth, I.; Karfunkel, H. R. *Angew. Chem.* **1994,** 106, 453.

12. Schick, G.; Hirsch, A.; Mauser, H.; Clark, T. *Chem. Eur. J.* **1996,** 2, 1537.

13. Lu, Q.; Schuster, D. I.; Wilson, S. R. *J. Org. Chem.* **1996,** 2, 4764.

14. Wiberg, K. B. *Tetrahedron* **1968,** 24, 1083.

15. Domingo, L. R.; Picher, M. T.; Arroyo, P.; Saez, J. A. *J. Org. Chem*. **2006,** 71, 9319.

16. Domingo, L. R.; Chamorro, E.; Pérez, P. *Eur. J. Org. Chem.* **2009,** 2009, 3036.

17. Domingo, L. R.; Aurell, M. J.; P**é**rez, P.; Contreras, R. *Tetrahedron* **2002,** 58, 4417.

18. P**é**rez, P.; Domingo, L. R.; Aurell, M. J.; Contreras, R. *Tetrahedron* **2003,** 59, 3117.

19. Pérez, P.; Domingo, L. R.; Aizman, A.; Contreras, R. Theoretical Aspects of Chemical Reactivity; Toro-Labbé, A., Ed.; Elsevier Science: Amsterdam, 2007; Vol. 19.

20. Jaramillo, P.; Domingo, L. R.; Chamorro, E.; Pérez, P. *J. Mol. Struct.* **2008,** 865, 68.

21. Gonzalez, C.; Schlegel, H. B. *J. Chem. Phys.* **1989,** 90, 2154.

22. Gonzalez, C.; Schlegel, H. B. *J. Phys. Chem.* **1990,** 94, 5523.

23. Reed, A. E.; Weinstock, R. B.; Weinhold, F. *J. Chem. Phys.* **1985,** 83, 735.

24. Reed, A. E.; Curtiss, L. A.; Weinhold, F. *Chem. Rev.* **1988,** 88, 899.

25. Frisch, M. J.; Trucks, G. W.; Schlegel, H. B.; Scuseria, G. E.; Robb, M. A.; Cheeseman, J. R.; Montgomery, J. J. A.; Vreven, T.; Kudin, K. N.; Burant, J. C.; Millam, J. M.; Iyengar, S. S.; Tomasi, J.; Barone, V.; Mennucci, B.; Cossi, M.; Scalmani, G.; Rega, N.; Petersson, G. A.; Nakatsuji, H.; Hada, M.; Ehara, M.; Toyota, K.; Fukuda, R.; Hasegawa, J.; Ishida, M.; Nakajima, T.; Honda, Y.; Kitao, O.; Nakai, H.; Klene, M.; Li, X.; Knox, J. E.; Hratchian, H. P.; Cross, J. B.; Adamo, C.; Jaramillo, J.; Gomperts, R.; Stratmann, R. E.; Yazyev, O.; Austin, A. J.; Cammi, R.; Pomelli, C.; Ochterski, J. W.; Ayala, P. Y.; Morokuma, K.; Voth, G. A.; Salvador, P.; Dannenberg, J. J.; Zakrzewski, V. G.; Dapprich, S.; Daniels, A. D.; Strain, M. C.; Farkas, O.; Malick, D. K.; Rabuck, A. D.; Raghavachari, K.; Foresman, J. B.; Ortiz, J. V.; Cui, Q.; Baboul, A. G.; Clifford, S.; Cioslowski, J.; Stefanov, B. B.; Liu, G.; Liashenko, A.; Piskorz, P.; Komaromi, I.; Martin, R. L.; Fox, D. J.; Keith, T.; Al-Laham, M. A.; Peng, C. Y.; Nanayakkara, A.; Challacombe, M.; Gill, P. M. W.; Johnson, B.; Chen, W.; Wong, M. W.; Gonzalez, C.; Pople, J. A. Gaussian 03 (Revision B.03), 2004.

26. Parr, R. G.; von Szentpaly, L.; Liu, S. *J. Am. Chem. Soc.* **1999,** 121, 1922.

27. Parr, R. G.; Pearson, R. G. *J. Am. Chem. Soc.* **1983,** 105, 7512.

28. Parr, R. G.; Yang, W. Density Functional Theory of Atoms and Molecules; Oxford University: New York, 1989.

29. Kohn, W.; Sham, L. *J. Phys. Rev.* **1965,** 140, 1133.

30. Domingo, L. R.; Chamorro, E.; Pérez, P. *J. Org. Chem.* **2008,** 112, 4615.

31. Truhlar, D. G.; Issacson, A. D.; Garett, B. C. In Generalized Transition State Theory, Vol 4 of Theory of Chemical Reaction Dynamics; CRC Press: Boca Raton, Florida, 1985.

32. Pilling, M. J.; Seakins, P. W. In Reaction Kinetics, 2 ed.; Oxford Science: Oxford, 1995.

33. Barreto, P. R. P.; Vilela, A. F. A.; Gargano, R. *Int. J. Quantum Chem.* **2005,** 103, 685.

Kindly visit:

7th Workshop on Computational Chemistry and Its Applications (7th CCA)
part of The International Conference on Computational Science
4 – 6 June, 2012, Omaha, Nebraska, USA

Workshop website: http://www.uom.ac.mu/Faculties/FOS/Chemistry/cca/

The International Conference on Pure and Applied Chemistry (ICPAC 2012)
2 – 6 July, 2012, Mauritius

Website: http://www.uom.ac.mu/icpac/2012/html/welcome.html